Local Anesthetics Disrupt Energetic Coupling between the Voltage-sensing Segments of a Sodium Channel

Yukiko Muroi and Baron Chanda

Department of Physiology, University of Wisconsin-Madison, Madison, WI 53706

Local anesthetics block sodium channels in a state-dependent fashion, binding with higher affinity to open and/or inactivated states. Gating current measurements show that local anesthetics immobilize a fraction of the gating charge, suggesting that the movement of voltage sensors is modified when a local anesthetic binds to the pore of the sodium channel. Here, using voltage clamp fluorescence measurements, we provide a quantitative description of the effect of local anesthetics on the steady-state behavior of the voltage-sensing segments of a sodium channel. Lidocaine and QX-314 shifted the midpoints of the fluorescence–voltage (F-V) curves of S4 domain III in the hyperpolarizing direction by 57 and 65 mV, respectively. A single mutation in the S6 of domain IV (F1579A), a site critical for local anesthetic block, abolished the effect of QX-314 on the voltage sensor of domain III. Both local anesthetics modestly shifted the F-V relationships of S4 domain IV toward hyperpolarized potentials. In contrast, the F-V curve of the S4 domain I was shifted by 11 mV in the depolarizing direction upon QX-314 binding. These antagonistic effects of the local anesthetic indicate that the drug modifies the coupling between the voltage-sensing domains of the sodium channel. Our findings suggest a novel role of local anesthetics in modulating the gating apparatus of the sodium channel.

The Journal of General Physiology

INTRODUCTION

Voltage-gated sodium channels play a central role in excitability in many cell types. Ionic currents through sodium channels generate the rising phase of an action potential. Several sodium channel–specific drugs prevent initiation and spread of action potentials by blocking sodium currents. Local anesthetics are a subset of sodium channel blockers that inhibit sodium currents in a use- and frequency-dependent manner (Strichartz, 1973). They bind with a higher affinity to the open and/or inactivated state of the channel (Hille, 1977). This state-dependent block of sodium currents by local anesthetics is reminiscent of the potassium channel block by internally applied quaternary ammonium compounds such as TEA ions (Armstrong, 1971; Armstrong and Hille, 1972). In both instances, ionic currents are blocked when the channels open. Gating current measurements in the Shaker potassium channel show that the gating charge movement is "immobilized" in the presence of internal TEA (Bezanilla et al., 1991). Blocking of the sodium channel pore by local anesthetics also modifies the movement of the gating charge in a similar fashion (Cahalan, 1978; Cahalan and Almers, 1979; Hanck et al., 1994). A third of the total gating charge is abolished in the presence of local anesthetics. These studies suggest that the binding of internal quaternary ammonium compounds to the sodium and potassium channels modulates the movement of their voltage sensors.

How does the binding of a local anesthetic affect the voltage sensors of the sodium channel? Structure–function studies have identified a cluster of residues in the S6 helices of domains III and IV of the sodium channel as constituents of a putative local anesthetic binding site (Ragsdale et al., 1994; Wang et al., 2001; Yarov-Yarovoy et al., 2002). Recent studies using unnatural amino acids show that the substitution of phenylalanine 1579 on the S6 of domain IV by cyclohexylalanine eliminates use-dependent block without modifying the gating properties of the channel (Ahern et al., 2008). A molecular modeling study suggests that the docking of a local anesthetic to the binding site prevents the closure of pore gates (Lipkind and Fozzard, 2005). Therefore, the local anesthetic may inhibit the movement of the gating charges indirectly by altering the pore conformation.

Gating current measurements in the human heart sodium channels show that when some of the charged residues in voltage sensors of domains III and IV are mutated, the fraction of the immobilized gating charge due to local anesthetic binding is reduced (Sheets and Hanck, 2003). The simplest interpretation is that these charged residues are the ones immobilized upon local anesthetic binding. The caveat, however, is that the mutations themselves could disrupt interactions between gating charges and the local anesthetic binding site,

Correspondence to Baron Chanda: bchanda@physiology.wisc.edu

Abbreviations used in this paper: BrMT, 6-bromo-2-mercaptotyptamine; F-V, fluorescence–voltage; Q-V, charge–voltage; TMR, tetramethylrhodamine; TMRM, TMR maleimide; TTX, tetradotoxin.

The Rockefeller University Press $30.00
J. Gen. Physiol. Vol. 133 No. 1 1–15
www.jgp.org/cgi/doi/10.1085/jgp.200810103

thereby reducing the extent of charge immobilization. To monitor the conformation of the individual voltage sensors directly, here we examined the effect of local anesthetics by using site-specific fluorescence measurements. We find that although all of the four voltage sensors are able to undergo the full extent of conformational rearrangements, their voltage dependence of fluorescence is altered in the presence of local anesthetics. The midpoint of the fluorescence–voltage (F-V) relationship of domain III is left-shifted by a large extent (65-mV shift for QX-314), indicating that the voltage-sensing segment of domain III is stabilized in the activated position. A relatively modest hyperpolarizing shift was observed in the F-V of domain IV (10 mV in QX-314). In contrast to the effects on domains III and IV, the voltage sensor of domain I was modestly stabilized in the closed state by QX-314. These opposing effects of QX-314 on the conformation of the voltage sensors were surprising. Perturbation experiments in conjunction with voltage clamp fluorescence measurements have shown that the four voltage sensors of the sodium channel essentially respond in a cooperative manner. For instance, mutations or site-specific toxins that stabilize a specific voltage sensor in an activated state also stabilize the other voltage sensors in the activated conformation (Chanda et al., 2004; Campos et al., 2007, 2008). Therefore, our findings reported here suggest that the local anesthetics, unlike the other Na^+ channel gating modifiers, disrupt the coupling between the voltage sensors of the sodium channel. We propose a new mechanism of action of the local anesthetic to account for the conformational changes in voltage-sensing segments of the sodium channel.

MATERIALS AND METHODS

Molecular Biology, Oocyte Expression, and Fluorophore Labeling

The α- and β-subunit of the rat skeletal muscle sodium channel (rNav1.4) cDNA were cloned into a pBSTA vector, which was optimized for oocyte expression (Chanda and Bezanilla, 2002). cRNAs of the α- and β-subunits were transcribed from NotI-linearized cDNA using a T7 RNA polymerase kit (Applied Biosystems) and coinjected at an ∼1:1 molar ratio (50 ng of the α-subunit and 10 ng of the β-subunit) for each oocyte. Oocytes were either purchased from NASCO or surgically removed from *Xenopus laevis* in a manner consistent with the guidelines of the Animal Care and Use Committee at the University of Wisconsin-Madison. The injected oocytes were incubated at 18°C for 3–4 d in an incubating solution (100 mM NaCl, 2 mM KCl, 1.8 mM $CaCl_2{\cdot}2H_2O$, 1 mM $MgCl_2{\cdot}6H_2O$, 5 mM HEPES, pH 7.2, 100 µM DTT, 0.2 mM EDTA, and 100 µg/ml gentamicin). The oocytes were labeled with 10 µM tetramethylrhodamine (TMR) maleimide (TMRM; Invitrogen) in a depolarizing solution (110 mM KCl, 1.5 mM $MgCl_2$, 0.8 mM $CaCl_2$, and 10 mM HEPES, pH 7.5) at 4°C for 30 min (Mannuzzu et al., 1996). 10 mM TMRM stock was prepared in DMSO and stored at −80°C. The labeled oocytes were washed and then stored in the external solution (115 mM NMG-Mes, 20 mM HEPES, and 2 mM $Ca[OH]_2$, pH 7.4) before recording.

Electrophysiology Setup and Recordings

All recordings were performed with a modified cut-open oocyte setup (CA-1B; Dagan Instruments) to measure currents and fluorescence under voltage clamp conditions (Cha and Bezanilla, 1998). The cut-open setup was placed on a stage of an upright microscope (BX50WI; Olympus). The light from a halogen lamp source (Newport Inc.) was filtered with a HQ535/50 bandpass filter and split using a Q565lp dichroic mirror (Chroma Technology Corp.). The emitted light was filtered with a HQ610/75 bandpass filter (Chroma Technology Corp.) and focused onto a PIN-020A Photodiode (UDT Technologies) by a condenser lens. The photodiode was connected to the headstage of an integrating Axopatch 1B patch clamp amplifier (MDS Analytical Technologies). To ensure that the photocurrent was within the dynamic range of the amplifier, additional current was fed into the summing junction of the headstage.

Intracellular solution contained 115 mM NMG-Mes, 20 mM HEPES, and 2 mM EGTA, pH 7.4. For ionic current measurement in the presence of lidocaine, the external sodium concentration was adjusted to 23 mM. For gating current measurements, 10 µM tetradotoxin (TTX; Sigma-Aldrich) was added to the extracellular solution in the top chamber. Lidocaine was prepared both in the external and internal solutions. QX-314 (Sigma-Aldrich) was prepared in the internal solution.

Data Acquisition and Analysis

Electrical and fluorescence signals were sampled at 250 kHz with a Digidata 1440 interface (MDS Analytical Technologies). For ionic current measurements, linear leak and membrane capacitive current were subtracted online using a P/4 procedure with a subtraction holding potential of −130 mV. Each fluorescence recording represents an average of 10 traces generated by a 20-ms test potential from −120 mV after a 20-ms conditioning pulse at −10 mV (see pulse protocols in the figures). Ionic current, gating current, and fluorescence intensity signals were low-pass filtered at 20 kHz. For steady measurements like F-V curves, the data were subsequently low-pass filtered offline at 5 kHz. The interval between the conditioning pulse and the test pulse was 100 ms. The conditioning pulse ensured that the lidocaine block of the sodium current was complete. Fluorescence intensity decay due to photobleaching was corrected by fitting the data before the pulse to a straight line and subtracting it from the full record. Fluorescence and electrophysiological data were acquired using Clampex (MDS Analytical Technologies), and analysis was performed with Clampfit (MDS Analytical Technologies) and Excel (Microsoft). The figures were prepared using Origin software (MicroCal) or PowerPoint (Microsoft). Prism (GraphPad Software, Inc.) was used for statistical analysis. A one-way ANOVA and *t* tests were used to determine the significance of the differences in the gating currents and fluorescence change.

Gating charge–voltage (Q-V) relationships or F-V relationships in Figs. 2 C, 3 B, 6 B, 7 C, and 8, and Fig. S3 (available at http://www.jgp.org/cgi/content/full/jgp.200810103/DC1), were fitted to a single Boltzmann distribution:

$$Q/Q_{max}(V) \text{ or } F/F_{max}(V) = 1 \,/\, (1 + \exp(-ze(V - V_m)/KT)),$$

where z is the apparent valence and V_m is the half-maximal voltage. K is the Boltzmann constant, T is the temperature, and e is the electronic charge. Both fluorescence intensities and gating charge were normalized to the maximum value, which was typically obtained at +50 mV, unless otherwise noted.

Kinetic Models

For the model shown in Fig. S2, the steady-state F-V curves for each subunit were generated by assuming that only transitions

from R to A give rise to fluorescence signals. Therefore, the fluorescence of the X subunit corresponds to:

$$FL\ [X] = X_A Y_R + X_A Y_A + X_A Y_O + X_O Y_R + X_O Y_A + X_O Y_O. \quad (1)$$

Because of conservation of mass, Eq. 1 can be rearranged to:

$$FL\ [X] = 1 - (X_R Y_R + X_R Y_A + X_R Y_O). \quad (2)$$

K_1 was used to represent the equilibrium constant of the R→A transition of subunit X, K_2 was used for the equilibrium constant for the R→A transition of subunit Y, K_3 was used for the equilibrium constant of the A→R transition for subunit X, and K_4 was used for the A→R transition for subunit Y. We can obtain the following expression of $X_R Y_R$, $X_R Y_A$, and $X_R Y_O$ in terms of equilibrium constants:

$$X_R Y_R = \frac{1}{(1 + K_1 + K_2 + K_2 \cdot K_4 + K_1 \cdot K_2 \cdot K_3 + K_1 K_2 K_4 + n \cdot K_1 K_2 K_3 K_4)}$$

$$X_R Y_A = \frac{1}{(1 + K_1 + K_4 + k_1 \cdot K_4 + K_1 K_3 + \frac{K_1}{K_2} + \frac{1}{K_1} + \frac{K_1 K_3}{K_2} + n \cdot K_1 K_3 K_4)}$$

$$X_R Y_O = \frac{1}{(1 + K_1 + \frac{1}{K_4 \cdot K_2} + \frac{K_1}{K_4} + \frac{K_1 \cdot K_3}{K_4} + \frac{K_1}{K_2 \cdot K_4} + \frac{K_1 \cdot K_3}{K_2 \cdot K_4} + n \cdot K_1 K_3)}$$

The fluorescence of subunit X is obtained by substituting $X_A Y_R$, $X_R Y_A$, and $X_R Y_D$ into Eq. 2. Similar expression can be derived for fluorescence due to the Y subunit (FL [Y]).

The equilibrium constants K_1 and K_2 are voltage dependent; therefore:

$$K(V) = e^{\left(\frac{-z.q.(V-Vm)}{KT}\right)} \quad (3)$$

where z is the apparent valence of voltage sensor and was set to 1 for these simulations. Eq. 3 was used to determine K_1 (subunit X) and K_2 (subunit Y) using the input V_m values shown in Table IV and Table S1 (available at http://www.jgp.org/cgi/content/full/jgp.200810103/DC1).

Online Supplemental Material

Fig. S1 shows control experiments to examine the direct effect of lidocaine on TMRM. Fig. S2 is a Markov model of a hypothetical channel with two subunits; each subunit undergoes two sequential transitions. Simulated F-V curves based on this model are shown in Fig. S3. The input parameters to generate the curves are listed in Table S1. The online supplemental material is available at http://www.jgp.org/cgi/content/full/jgp.200810103/DC1.

RESULTS

To investigate the effect of local anesthetics on the conformational dynamics of the voltage sensors of a sodium channel, we labeled substituted cysteines in each of the S4s with a fluorescent probe, TMR. The labeled residues correspond to positions S216, S660, L1115, and S1436 (Fig. 1 A) in domains I, II, III, and IV, respectively, in the rat skeletal muscle sodium channels (rNav1.4). Previous work by Chanda and Bezanilla (2002) established that the time course of early fluorescence changes from probes attached to these residues correlates with the movement of the gating charge. Here, using a similar combined fluorescence and electrophysiological approach, we have examined the effects of two local anesthetics, lidocaine and QX-314 (Fig. 1 B), on the conformational dynamics of the voltage-sensing segments of the rNav1.4 channel.

Lidocaine Modifies the Movement of Gating Charge in the Rat Skeletal Muscle Sodium Channel

Lidocaine is a tertiary amine and can exist as an equilibrium mixture of cationic and neutral forms, with a pKa of 7.9 (at 26°C). At physiological pH, lidocaine is membrane permeant and shows both use-dependent and resting-state block. The cationic form of lidocaine is a more potent use-dependent blocker compared with the

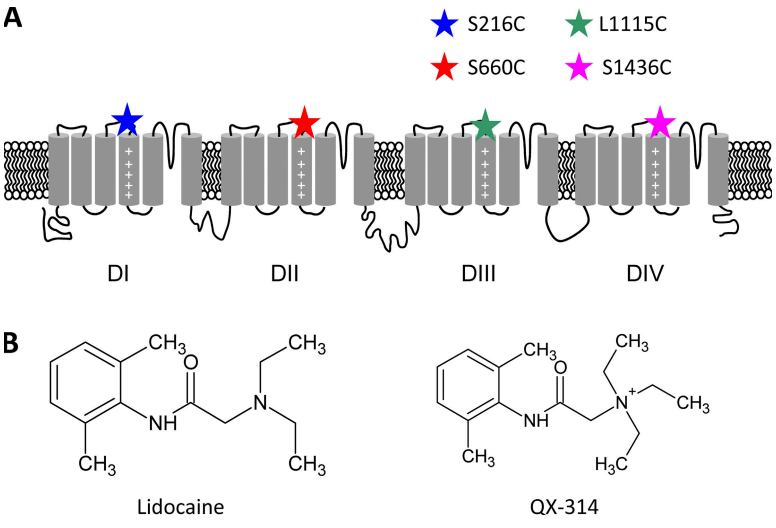

Figure 1. A schematic of the sodium channel and chemical structures of local anesthetics. (A) A schematic diagram of the α-subunit of the sodium channel. Positions of the substituted cysteines at S216 (domain I [DI]), S660 (domain II [DII]), L1115 (domain III [DIII]), and S1436 (domain IV [DIV]) are depicted as colored stars. (B) Chemical structure of lidocaine and QX-314.

neutral forms (Schwarz et al., 1977). The dissociation constant for use-dependent and resting-state block of rNav1.4 channels expressed in *Xenopus* oocytes by lidocaine was estimated to be 100 µM and 1 mM, respectively (Makielski et al., 1999). Representative ionic currents from the wild-type channels elicited by repetitive depolarizing pulses in the presence of 10 mM lidocaine show that block is nearly complete at the end of the first depolarizing pulse (Fig. 2, A and B). Fig. 2 B shows the normalized current amplitudes of the wild-type and mutant channels plotted with respect to the pulse number in the presence of lidocaine. These experiments demonstrate that a single depolarizing pulse is sufficient to block the rNav1.4 channels completely after the addition of 10 mM lidocaine.

Next, we examined the effect of lidocaine on the gating currents of the wild-type and mutant sodium channels. Local anesthetics decrease the maximal gating charge of sodium channels from the squid axon and cardiac muscles by ~30% and slightly shift their voltage dependence toward a hyperpolarizing direction (Hanck et al., 1994, 2000; Cahalan, 1978; Cahalan and Almers, 1979). Fig. 2 C shows the Q-V relationship of the wild-type sodium channels in the presence of 10 mM lidocaine. The gating currents were obtained after blocking ionic currents with TTX. In the wild-type channels, lidocaine reduced the maximal gating charge by 25% (Table I). A similar reduction in the gating change in the presence of lidocaine was also observed for the cysteine mutants. The extent of modification of gating charge in the rNav1.4 is comparable to those observed in the human heart sodium channels (Sheets and Hanck, 2003).

Lidocaine Selectively Modifies Conformational Dynamics in the Voltage-sensing Domains

The effect of lidocaine on the movement of individual voltage sensors was monitored by labeling substituted cysteine mutants with TMR and measuring the fluorescence intensities before and after the application of 10 mM lidocaine. Fig. 3 A shows the fluorescence traces obtained at varying pulse potentials. Note that the fluorescence traces were recorded after a single conditioning pulse to −10 mV to ensure that the sodium channels were fully blocked by lidocaine. The normalized fluorescence change (ΔF/F) varied from 0.5 to 2%. The largest effect of lidocaine was seen on the fluorescence from the S4 of domain III. Compared with other domains, the fluorescence signals were saturated at depolarizations beyond −70 mV, suggesting that the voltage-dependent movement of S4 of domain III was shifted to hyperpolarized potentials.

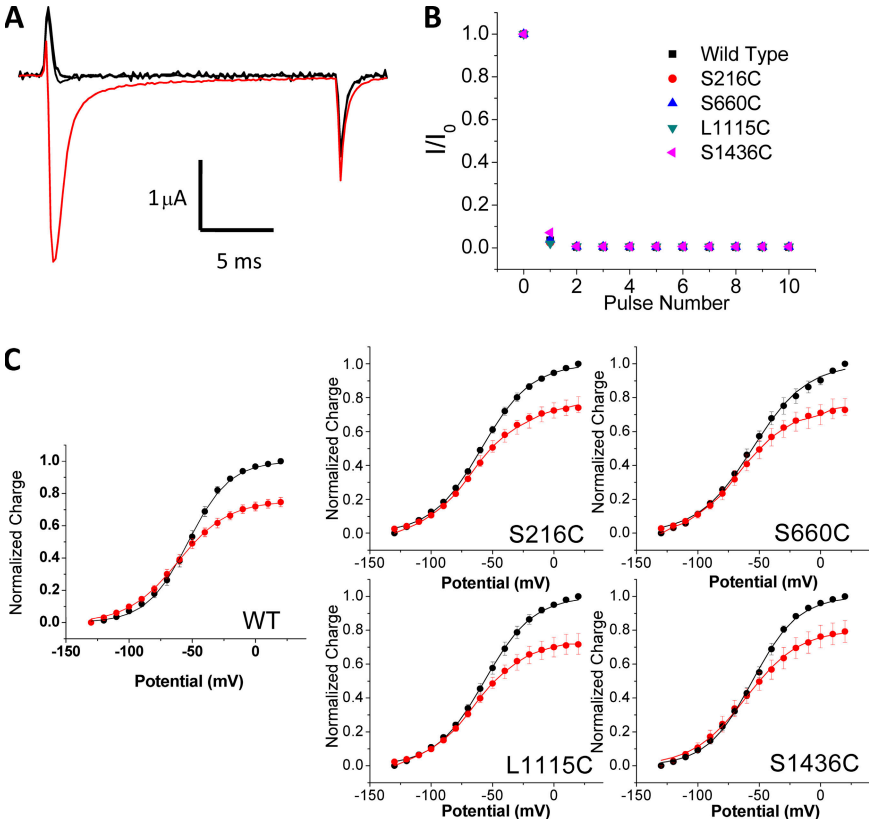

Figure 2. The effect of saturating concentrations of lidocaine on ionic and gating currents of the sodium channel. (A) Development of ionic current block in the presence of 10 mM lidocaine in wild-type sodium channels. The ionic currents were elicited by pulsing to −10 mV for 20 ms with a prepulse to −120 mV for 50 ms. Red trace shows the currents obtained before the addition of lidocaine. A family of 100 traces was recorded by pulsing at 10 Hz 5 min after lidocaine application (in black). Ionic current blockade was nearly complete after the first pulse. These recording were obtained with 23 mM sodium in the external solution. (B) Fractional ionic current block of wild-type and mutant sodium channels elicited by repetitively pulsing to −10 mV (10 Hz frequency) after the addition of 10 mM lidocaine. The currents were normalized to the ones obtained before the addition of lidocaine. (C) Effect of 10 mM lidocaine on the steady-state Q-V relationships of wild-type and mutant channels. The dark lines and symbols show the data in control (with TTX and no lidocaine), while the red lines and symbols show the data after lidocaine application. Filled circles represent the mean ± SE of at least four independent experiments, and lines represent the best fits of the averaged data to a Boltzmann function. Measured gating charges at each potential were normalized to the maximum charge determined for each oocyte without lidocaine.

TABLE I

The Effect of 10 mM Lidocaine on Gating Charge of Wild-type and Mutant Sodium Channels

		Control (TTX)		TTX and lidocaine (5 min)		Remaining gating charge
Mutants	*n*	Midpoint	Slope	Midpoint	Slope	
		V_m	e_0	V_m	e_0	%
WT	9	−53.4 ± 2.4	1.62 ± 0.06	−61.3 ± 2.2[a]	1.32 ± 0.02	75.1 ± 2.7
S216C	5	−56.0 ± 1.8	1.25 ± 0.03	−64.0 ± 1.0[a]	1.28 ± 0.03	75.2 ± 4.5
S660C	4	−55.2 ± 3.2	1.17 ± 0.09	−64.0 ± 2.1[a]	1.26 ± 0.05	74.0 ± 5.8
L1115C	5	−56.4 ± 2.8	1.30 ± 0.05	−64.5 ± 2.6	1.32 ± 0.02	72.6 ± 6.2
S1436C	4	−55.6 ± 2.4	1.37 ± 0.01	−60.9 ± 3.3[a]	1.19 ± 0.04	80.1 ± 6.6

The Boltzmann parameters from a first-order fit of the Q-V relationships and remaining gating charge after lidocaine application in different mutants. All measurements were recorded in the presence of TTX. Data represent the mean ± SE of four to nine independent experiments (*n*).

[a]Significance ($P < 0.05$) was determined for paired *t* test for each mutant channel before and after the application of lidocaine. A one-way ANOVA was used to compare the differences in midpoints and remaining values of the mutants to the wild-type, followed by a post-hoc Dunnett's test. Those differences were not statistically significant.

Fig. 3 B shows the plots of normalized F-V relationships obtained from labeled mutants before and after the addition of 10 mM lidocaine. The F-V curve of the domain III voltage sensor showed a dramatic leftward shift ($\Delta V_m = 57$ mV) in the presence of lidocaine (Table II). The F-V curve of the domain IV voltage sensor showed a small (ΔV_m = 10 mV) but significant leftward shift. In addition, the apparent slope was reduced from 1.2 to 1.0 e_o, suggesting that some or all of the domain IV gating charges move to a lesser extent across the electric field compared with the unmodified channels. In contrast, the F-V curves of domains I and II were not significantly different upon lidocaine binding. Previous studies have shown that site-specific perturbations that alter the voltage-dependent movement of the S4 of domain III also affect the movement of the voltage sensors in other domains (Chanda and Bezanilla, 2002). Therefore, it was surprising that a large leftward shift in the voltage-dependent movement of the S4 of domain III was not propagated to voltage-sensing segments of domains I and II.

The absolute magnitudes of decrease in the fluorescence signals were found to be highly variable upon the addition of lidocaine. These decreases ranged from 1 to 25% between different oocytes expressing the same construct and were not statistically correlated with the shifts in the F-V curve (unpublished data). We suspect that this variability in fluorescence signals is either due to a nonspecific effect of lidocaine on the channels or a drift in the focus during perfusion. We also considered the possibility that lidocaine may interact and quench the rhodamine fluorescence directly. Polynuclear aromatic compounds, such as TMR, are known to interact with amine groups and form a charge–transfer complex (Rehm and Weller, 1970; Kumbhakar et al., 2004). Previously, tetracaine and procaine, but not lidocaine, were shown to quench fluorescence of anthracene-based fluorophores (Koblin et al., 1975). We wondered whether lidocaine is a more effective quencher of rhodamine fluorescence in a lipid environment because rhodamine has a longer lifetime in a nonpolar environment. This hypothesis was tested by measuring the quenching of a membrane-localized fluorophore, octadecylrhodamine, in oocytes by lidocaine (Fig. S1). Our measurements show that increasing concentrations of lidocaine had no effect on rhodamine fluorescence in a bilayer environment.

Molecular modeling based on structure–function studies suggests that lidocaine binds to conserved residues in the S6 helices of domains III and IV (Lipkind and Fozzard, 2005). Mutation of a single site in the S6

TABLE II

F-V Relationships before and after Lidocaine Application

		Control		10 mM lidocaine (5 min)	
Mutants	*n*	Midpoint	Slope	Midpoint	Slope
		V_m	e_0	V_m	e_0
S216C (DI)	6	−68.4 ± 3.6	1.02 ± 0.08	−65.6 ± 3.6	1.16 ± 0.16
S660C (DII)	6	−67.7 ± 1.5	1.04 ± 0.03	−68.6 ± 4.5	1.11 ± 0.04
L1115C (DIII)	6	−70.2 ± 2.9	1.51 ± 0.1	−127.1 ± 4.5[a]	1.36 ± 0.18
S1436C (DIV)	12	−69.8 ± 2.3	1.23 ± 0.06	−79.7 ± 3[a]	1.04 ± 0.04[a]
L1115C (with TTX)	5	−75.7 ± 3.6	1.10 ± 0.2	−122.5 ± 4.3[a]	1.79 ± 0.6

Boltzmann parameters from a first-order fit of F-V relationships before and after lidocaine application. Data represent the mean ± SE of 5–12 independent experiments (*n*).

[a]Significance ($P \leq 0.01$) was determined using a paired *t* test for each mutant before and after the addition of lidocaine. The parameters of L1115C mutant channels with and without TTX did not show any statistically significant differences when compared using an unpaired *t* test.

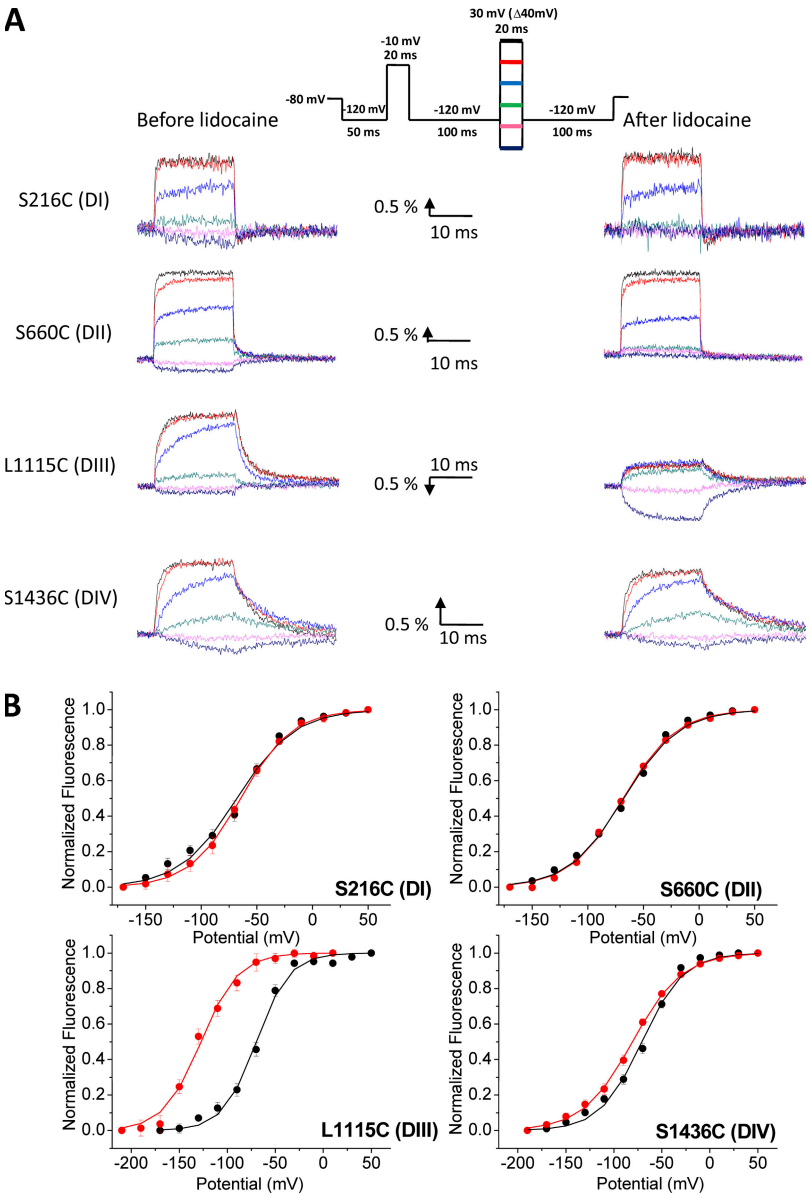

Figure 3. The effect of lidocaine on the on the voltage-dependent fluorescence of labeled sodium channel domains. (A) Time-dependent fluorescence changes from TMR-labeled S216C, S660C, L1115C, and S1436C channels before (left) and after (right) 10 mM lidocaine application. Inset shows the pulse protocol. Each trace was obtained by averaging 10 trials with an interval of 1 s between pulses. The y axis in the scale bar represents percent fluorescence change (ΔF/F). L1115C fluorescence traces were inverted for comparison. (B) Steady-state F-V relationship of TMR-labeled S216C, S660C, L1115C, and S1436C channels before (black) and after (red) a 10-mM lidocaine application. Circles represent the means ± SE of at least five independent experiments, whereas the lines represent the best fits of the averaged data to a single Boltzmann function.

of domain IV abolishes use-dependent block. Our findings, however, show that compared with domain III, lidocaine may have little effect on the movement of the S4 of domain IV. It is possible that the local anesthetic in the pore modestly stabilizes the S6 segment of domain IV. Alternatively, the S6 of domain IV is highly stabilized in activated conformation by local anesthetic binding, but its coupling with the domain IV voltage sensor is not tight, allowing the voltage sensor to return with a limited energetic cost.

Lidocaine produces a relatively minor shift in the Q-V relationship of the sodium channels, whereas the F-V of the domain III voltage sensor was shifted by >50 mV. We consider the possibility that TTX affects lidocaine-induced fluorescence shift. Early gating current measurements in the squid sodium channel have suggested that the TTX may allosterically increase the binding affinity of charged lidocaine derivatives (Cahalan, 1978; Cahalan and Almers, 1979). The Q-V, but not F-V, curves were obtained by blocking ionic currents with TTX. Therefore, we compared the F-V curves obtained before and after lidocaine in L1115C channels previously blocked by TTX (Table II). Our experiments show that the TTX does not significantly alter the lidocaine-induced leftward shift in the F-V curve. These results are consistent with similar findings in the cardiac channels (Hanck et al., 1994).

Lidocaine Modifies Both Fast and Slow Fluorescence Signals of the S4 of Domain III

Fluorescence measurements on the sodium channel show that the voltage sensors undergo at least two gating transitions. The early gating transitions correlate with the movement of the gating charge and are likely

to account for the majority of the charge movement (Chanda and Bezanilla, 2002). To test whether lidocaine selectively inhibits one of the fluorescence components, we examined the voltage-dependent fluorescence changes from another position (S1113) on the voltage sensor of domain III. The early component of fluorescence at this position corresponds to an increase in fluorescence intensity, whereas the late component corresponds to a decrease in fluorescence intensity (Chanda and Bezanilla, 2002). Thus, both components in the fluorescence signals can be easily resolved. Fig. 4 A shows a representative family of voltage-dependent fluorescence traces from S1113C before and after the addition of lidocaine. The F-V curve shows a clear initial increase corresponding to the early component, followed by a decrease in fluorescence as the late component predominates at more depolarized potentials (Fig. 4 B). The transition point in the F-V curve shows a 40-mV leftward shift in the presence of lidocaine. Thus, both the early and late components were equally modified by lidocaine and also suggest that the voltage-dependent shift observed in the presence of lidocaine likely reflects the general behavior of the voltage sensor of domain III.

QX-314 Has a More Pronounced Effect on the Voltage Sensors Compared with Lidocaine

QX-314 is a quaternary amine derivative of lidocaine generated by *N*-ethyl substitution on the amine group (Fig. 1 B). At saturating concentrations, QX-314 blocks sodium currents predominantly in a use-dependent manner. Furthermore, QX-314 is membrane impermeant and unlikely to perturb the lipid bilayer surrounding the voltage sensors. Fig. 5 shows a representative use-dependent block of potassium currents through the sodium channel by QX-314. Ionic currents were recorded 10 min after the addition of QX-314 to the internal chamber of the cut-open oocyte setup. Typically, 200 pulses were sufficient to block outward currents completely in the presence of 3 mM QX-314. The remaining transient current after the block was the gating current. This was confirmed by obtaining the current integrals, which were saturated at depolarized potentials for gating currents.

Before recording signals from QX-314–modified channels, we applied a train of depolarizing pulses (10 Hz, −10 mV) to ensure a complete block of ionic currents. This was immediately followed (within a 2-s interval) by a protocol to monitor fluorescence signals from modified channels (Fig. 3 A, inset). Fig. 6 A shows representative voltage-dependent fluorescence signals over time from the labeled cysteine mutants. Analogous to lidocaine, the fluorescence change from the S4 of domain III was saturated at depolarizations beyond −70 mV, indicating that the voltage dependence of fluorescence changes were shifted toward a hyperpolarized direction.

Plots of the F-V relationships show that L1115C and S1436C were left shifted upon QX-314 block of the sodium channels (Fig. 6 B). The midpoints of the F-V curve of the domain III were left-shifted by at least 65 mV, whereas that of domain IV was left-shifted by 16 mV

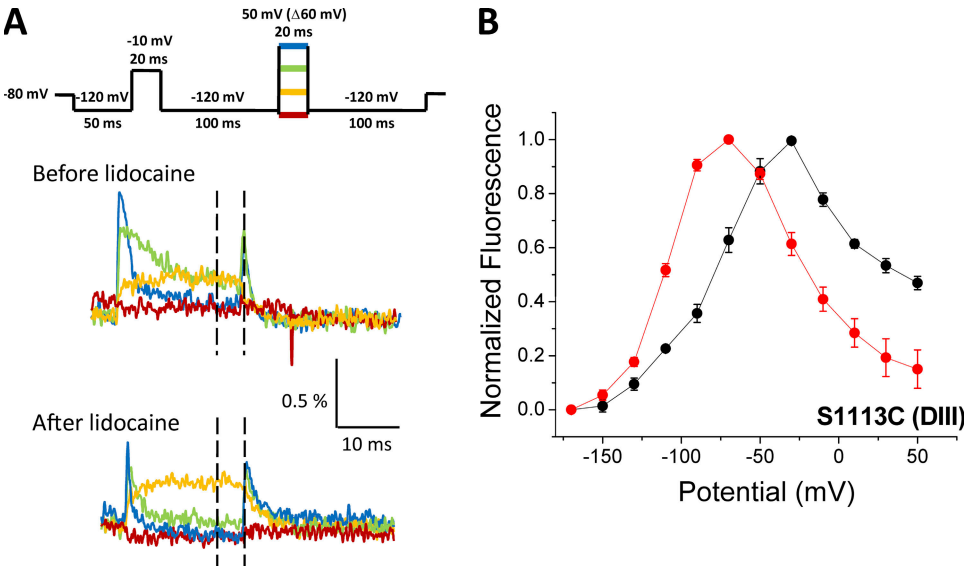

Figure 4. The effect of lidocaine on an alternate site in the S4-DIII of the sodium channel. (A) Effect of 10 mM lidocaine on voltage-dependent fluorescence changes from TMR-labeled S1113C before (top) and after (bottom) lidocaine application. Inset shows the pulse protocol. The y axis in the scale bar represents percent fluorescence change (ΔF/F). The traces were obtained by averaging 10 trials per test potential with an interval of 1 s between pulses. (B) F-V relationships from TMR-labeled S1113C mutants before (black) and after (red) a 10-mM lidocaine application. The averaged fluorescence intensity in the last 3 ms of the voltage pulse was measured (marked with dashed lines in A). These fluorescence intensity changes were normalized to the maximum fluorescence change. Circles represent the means ± SE of five independent experiments, and the line represents the best fit of the averaged data to a single Boltzmann function.

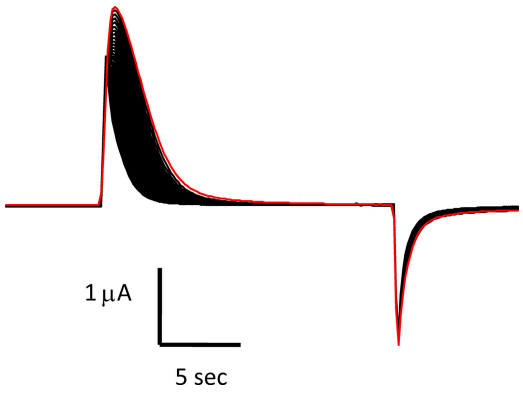

Figure 5. The effect of saturating concentrations of QX-314 on ionic currents of the sodium channel. Use-dependent block of outward potassium currents through the sodium channel obtained by repetitively pulsing in the presence of 3 mM QX-314. Red trace represents the current in the absence of QX-314. 10 min after the application of 3 mM QX-314 to the internal solution, ionic currents (black) were recorded by repetitive pulses (10 Hz frequency) to −10 mV for 20 ms after a −120-mV prepulse for 50 ms.

(Table III). Note that the F-V curve of domain III does not saturate even at −210 mV, suggesting that the 65-mV left shift is likely to be a low estimate. More remarkably, the F-V curves of the S4s of domains I and II were right-shifted when the channels were blocked by QX-314. The depolarizing shift in the S4 of domain I was statistically significant ($P \leq 0.01$). These findings indicate that QX-314 modifies the interactions between the voltage sensors of the sodium channel, such that some of the domains (III and IV) are stabilized while others (domain I) are destabilized in the activated conformation.

A Residue in the Pore Is Essential for Use-dependent Block and Local Anesthetic–induced Shift in Movement of the Voltage Sensor of Domain III

We consider the possibility that local anesthetics affect the movement of the voltage sensors by either altering the membrane properties or by interacting with the voltage sensor. To address this issue, we monitored the shifts in the fluorescence of domain III while simultaneously recording the development of use-dependent block. Fig. 7 A shows the normalized peak current amplitudes plotted along with normalized fluorescence amplitudes obtained by repetitively pulsing to +50 mV from −120 mV at a 10-Hz frequency after the addition of QX-314. With this pulse protocol, a large leftward shift in the voltage-dependent fluorescence signals of the S4 of domain III is manifested as a decrease in fluorescence amplitude. The plot shows that within experimental limits both ionic currents and fluorescence signals decrease proportionately, indicating that the voltage sensor modification correlates with QX-314 block of sodium currents.

A recent study in the cardiac sodium channel has shown that a mutation of a conserved phenylalanine (equivalent to F1579 in rNav1.4) in the S6 segment abolishes both use-dependent block as well as charge immobilization in the presence of local anesthetics (Sheets et al., 2008). We tested the effect of QX-314 interaction on S4 domain III fluorescence in F1579A mutant. Ionic currents from F1579A mutant did not show any significant use-dependent block when compared with those obtained before QX-314 addition (Fig. 7 B). The F-V of domain III voltage sensor in the mutant channel was unaltered upon the application of QX-314 (Fig. 7 C and Table III). These findings demonstrate that the modification of the voltage sensors is due to the use-dependent block of the sodium channel by QX-314.

DISCUSSION

Interaction of Local Anesthetic with the Pore Disrupts Energetic Coupling between the Voltage Sensors of the Sodium Channel

Local anesthetics bind preferentially to the sodium channel pore in the open state and reduce the total gating charge by ∼30% (Hille, 1977; Cahalan and Almers, 1979; Hanck et al., 1994). Using a voltage clamp fluorescence

TABLE III

F-V Relationships before and after QX-314 Application

		Control		3 mM QX-314 (10 min)	
Mutants	*n*	Midpoint	Slope	Midpoint	Slope
		V_m	e_0	V_m	e_0
S216C (DI)	5	−71.3 ± 3.0	1.03 ± 0.08	−60.4 ± 3.3[a]	1.45 ± 0.17[a]
S660C (DII)	5	−69.2 ± 1.6	0.95 ± 0.02	−58.8 ± 4.9	1.19 ± 0.12
L1115C (DIII)	9	−75.2 ± 1.02	1.43 ± 0.09	−140.0 ± 3.2[a]	1.05 ± 0.08[a]
S1436C (DIV)	5	−63.0 ± 1.5	1.46 ± 0.06	−79.8 ± 4.1[a]	1.09 ± 0.07[a]
L111C/F1579A	4	−62.9 ± 0.8	1.22 ± 0.07	−56.94 ± 2.5	1.39 ± 0.18

Boltzmann parameters from a first-order fit of F-V relationships before and after QX-314 addition. Data represent the mean ± SE of at least five independent experiments (*n*).

[a]Significance ($P \leq 0.01$) was determined using a paired *t* test for each mutant channel before and after the addition of QX-314.

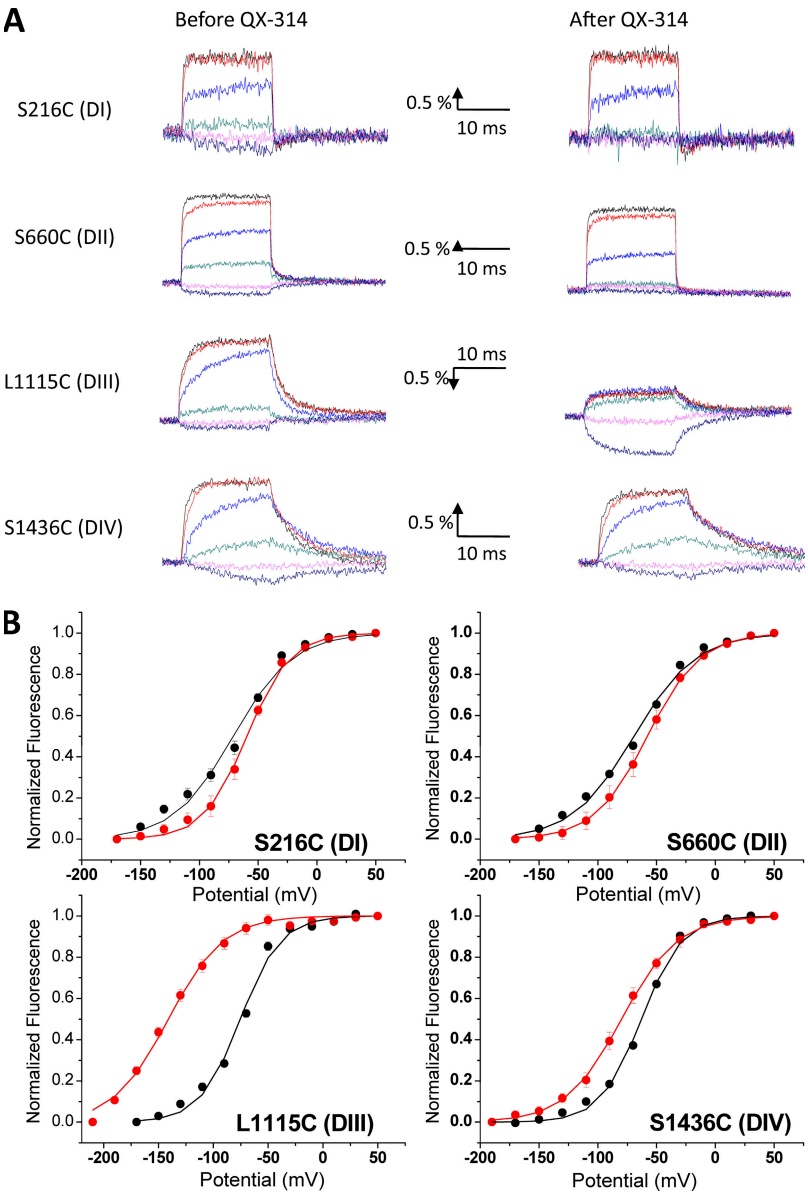

Figure 6. The effect of saturating concentrations of QX-314 on the voltage-dependent fluorescence of labeled sodium channel domains. (A) Time-dependent fluorescence changes from TMR-labeled S216C, S660C, L1115C, and S1436C channels are shown before (left) and after (right) the application of 3 mM QX-314. 10 min after the application of QX-314, oocytes were pulsed repetitively until ionic current block was complete (typically 200 pulses). Traces were obtained by averaging 10 trials per test potential with an interval of 1 s between pulses. The y axis in the scale bar represents percent fluorescence change ($\Delta F/F$). L1115C fluorescence traces were inverted for comparison. (B) Effect of 3 mM QX-314 on the steady-state F-V relationship of S216C, S660C, L1115C, and S1436C channels. Black and red traces represent the data before and after QX-314 application, respectively. Symbols represent the mean ± SE of at least five independent experiments, and lines represent the best fits of the averaged data to a single Boltzmann function. Steady-state fluorescence intensities at each potential were normalized to the maximum changes in fluorescence in each oocyte.

approach, we quantified the effect of local anesthetics on the movement of S4 segments of the sodium channel. We find that the permanently charged local anesthetic, QX-314, mainly stabilized the voltage sensors of domain III in an activated conformation. The voltage sensor of domain IV was slightly stabilized in the activated state. In contrast to the effects on domains III and IV, the voltage sensor of domain I was stabilized in the resting conformation. The voltage sensors of the rNaV1.4 channel were previously shown to be positively coupled to each other (Chanda et al., 2004; Campos et al., 2007). Stabilizing one of the voltage sensors in the resting state stabilizes the other voltage sensors of the sodium channel in the same conformation. Campos et al. (2007) have shown that β-scorpion toxin, which binds specifically to domain II of the sodium channel and traps it in an activated state, also stabilizes the voltage sensors of the other three domains in the activated state. In contrast to those gating-modifier toxins, local anesthetics have opposing effects on the different voltage sensors of the sodium channel. Thus, our findings indicate that local anesthetics modify the coupling between the voltage sensors of the sodium channel.

Scanning mutagenesis experiments suggest that the residues in the S6 segments of domains I, III, and IV play a crucial role in use-dependent block by local anesthetics (Ragsdale et al., 1996; Yarov-Yarovoy et al., 2001, 2002). A recent study using unnatural amino acids has shown that reducing the aromaticity of a highly conserved phenylalanine at position 1,579 abolished use-dependent block but had no effect on resting-state block (Ahern et al., 2008). Although there is no direct structural evidence, molecular modeling suggests that the aromatic ring of F1579 interacts with the alkylamonium

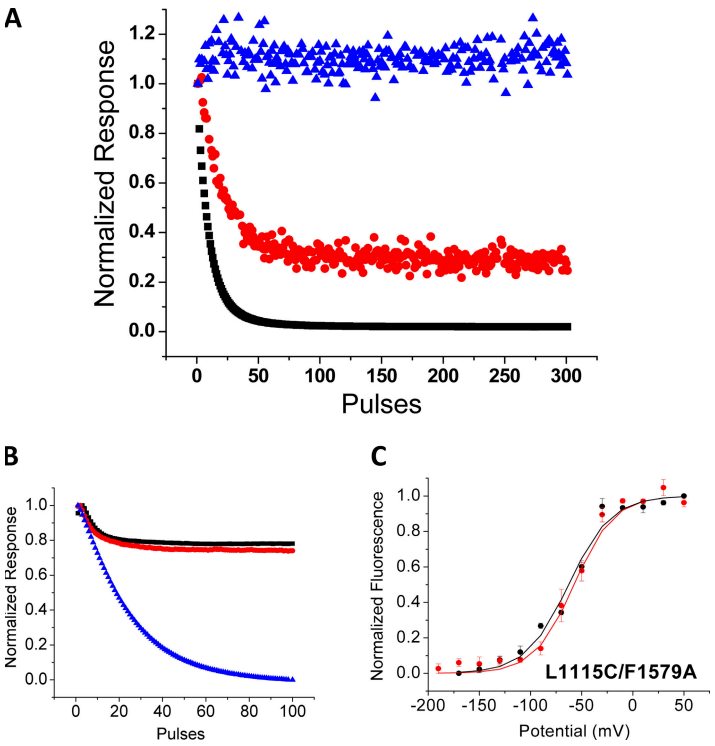

Figure 7. Correlations between use-dependent block of ionic currents and voltage-dependent fluorescence of S4-DIII. (A) A comparison of the development of use-dependent block of ionic current and shift in the voltage-dependent fluorescence of S4-DIII (L1115C). Shift in the voltage dependence of fluorescence manifests as a decrease in fluorescence amplitude when pulsed from −120 to +50 mV. Ionic currents and fluorescence signals were obtained by pulsing repetitively (10 Hz frequency) 10 min after the addition of QX-314. Black symbols represent ionic currents, which were normalized to the current obtained before QX-314 application. Red symbols represent fluorescence intensity, which was normalized to the fluorescence signals before the addition of QX-314. Blue symbols represent fluorescence intensity without QX-314 application obtained in an independent experiment. Large deviations in fluorescence intensities occurred when the capacitor in the amplifier headstage discharged in the middle of a trace. Those datasets were eliminated from the final plots. (B) A comparison of use-dependent block in the L1115C and L1115C/F1579A double-mutant sodium channel. Use-dependent block of outward potassium currents was elicited by repetitively pulsing in the presence of 3 mM QX-314. Black symbols represent the current in the absence of QX-314 in the L1115C/F1579A channel. 10 min after the application of 3 mM QX-314 to the internal solution, ionic currents of L1115C/F1579A channel (red symbols) were recorded by repetitive pulses (10 Hz frequency) to −10 mV for 20 ms after a −120-mV prepulse for 50 ms. Blue symbols represent the current in the presence of QX-314 in the L1115C channel, obtained with the same protocol pulse. (C) Effect of QX-314 on the voltage-dependent fluorescence of the L1115C/F1579A mutant channel. F-V relationships from TMR-labeled L1115C/F1579A mutants before (black) and after (red) a 3-mM QX-314 application (after 100 depolarizing pulses at 10 Hz frequency). These fluorescence intensity changes were normalized to the maximum fluorescence change. Circles represent the means ± SE of four independent experiments, and the line represents the best fit of the averaged data to a single Boltzmann function.

group of the local anesthetic (Lipkind and Fozzard, 2005). Gating charge measurements show that mutating this site also abolishes charge immobilization by lidocaine, indicating that the resting-state block does not affect the movement of the voltage sensor (Sheets et al., 2008). We find that mutating this residue to alanine also eliminates the QX-314–induced shifts in the voltage-dependent movement of domain III. Collectively, these findings are consistent with the notion that the binding of the local anesthetic to a site in the pore of the sodium channel modifies the gating behavior of the channel.

The effect of QX-314 on the voltage sensors of the sodium channel was more pronounced compared with lidocaine. The voltage sensors of domain I showed a modest rightward shift upon the addition of QX-314, whereas lidocaine had no effect on the movement of this voltage sensor. Also, lidocaine had a smaller effect on the movement of the voltage sensor of domain III compared with QX-314. These differences between QX-314 and lidocaine on the voltage sensors of the sodium channel are likely to be due to the differences in the extent of use-dependent block. QX-314, which has a quaternary ammonium group, is a more potent use-dependent blocker than lidocaine (Schwarz et al., 1977). Nonetheless, we cannot rule out the possibility that the additional ethyl group on QX-314, compared with lidocaine, causes a larger perturbation in the sodium channel.

In Relation to Previous Studies of Local Anesthetics on Sodium Channel Gating

Many pore blockers such as TEA that block the voltage-dependent ion channels in a use-dependent fashion also modify the movement of the gating charge (Cahalan and Almers, 1979; Bezanilla et al., 1991). The total gating charge is reduced by ∼40% upon the addition of a saturating concentration of local anesthetic (Hanck et al., 2000). In an effort to identity the specific voltage sensors, Sheets and Hanck (2003) examined the effect of mutating voltage sensor charges on the fraction of immobilized gating charge. Neutralization of the charge-carrying residues in domains III and IV reduced the immobilized fraction, suggesting that those voltage sensors are affected upon local anesthetic binding. Nonetheless, there are some significant limitations of this approach. Mutations may reduce the fraction of immobilized gating charge by disrupting the interaction between the voltage-sensing domain and the local anesthetic binding site. Furthermore, these measurements do not directly measure the movement of individual voltage sensors and, therefore, cannot provide a quantitative description of the effect on their stability and conformation.

According to the Modulated Receptor model, the local anesthetic stabilizes the sodium channel in the inactivated state (Hille, 1977). Our fluorescence data show that the local anesthetic has a relatively modest effect on domain IV compared with domain III. This was particularly surprising in light of the evidence from several studies suggesting that the voltage sensor of domain IV plays a crucial role in the inactivation of the sodium channel (Chen et al., 1996; Horn et al., 2000; Hanck and Sheets, 1995; Sheets and Hanck, 1995). Thus, our fluorescence recordings would suggest that the local anesthetic is unlikely to have a strong preference for the inactivated state of the sodium channel. Our observations are consistent with cysteine accessibility measurements showing that the lidocaine binding did not affect the conformational changes associated with the IFM motif, a region known to be crucial for inactivation (Vedantham and Cannon, 1999).

Perhaps the most surprising finding of our study was that the addition of QX-314 caused a rightward shift in the voltage-dependent movement of domain I compared with the large leftward shift in domain III. These effects were not observed in the gating current studies using lidocaine (Sheets and Hanck, 2003). Voltage clamp fluorescence measurements with sodium channel gating modifiers such as site III and site IV toxins show that the voltage dependence of all four domains was shifted in the same direction by the toxins (Campos et al., 2007, 2008). Thus, the local anesthetics appear to be unique among the family of sodium channel gating modifiers. In addition to selectively modifying the movement of specific voltage sensors, local anesthetics disrupt the coupling between the domains of the sodium channel. Recently, Sack and Aldrich (2006) used sigmoidicity analysis of ionic currents to demonstrate that a gastropod toxin, 6-bromo-2-mercaptotyptamine (BrMT), induces intersubunit cooperativity in the early gating transitions of the Shaker potassium channel. This would suggest that voltage sensors of the potassium channel become coupled to each other in the presence of the toxin. Thus, both BrMT and local anesthetics modify the coupling between the subunits or domains of voltage-gated ion channels.

Our fluorescence measurements also show that the activated state of domain III is highly stabilized but, in contrast to the gating current data, the voltage-sensing segment of domain III is still able to undergo the full extent of conformational change. Because the gating current data were obtained by subtracting the linear capacity transients at a holding potential of −150 mV, we considered the possibility that a significant fraction of the total gating charge is subtracted when the Q-V shifts to a more hyperpolarized potential. However, gating current measurements with a prepulse from −170 mV and a subtraction holding potential at +40 mV did not alter the fraction of the reduced gating charge (not depicted). This suggests that the gating charge reduction was unlikely to be a subtraction artifact.

The differences between gating current and fluorescence data could be due to several reasons. The relationship between the amplitude of fluorescence signal and the size of the gating currents is poorly defined. Gating current depends on the amount of charge translocated across the electric field, whereas the size of a fluorescence signal depends on the extent of change in the surrounding environment, such as a polarity and proximity to quenching groups. One possible scenario to account for the differences between the gating current and fluorescence data is that the binding of the drug modifies the conformation of the channel, thereby distorting the electric field. Consider, for instance, that the electric field is focused over a distance of 5 Å and a gating particle moving over this distance carries 1 e_o unit of charge. If, because of a change in the structure, the electric field becomes less focused and is spread over a larger distance, say 10 Å, the effective charge would become 0.5 e_o. The amplitude of S4 fluorescence may remain the same in both cases. Alternatively, the fluorescence signals from probes attached to the top of the S4 segment may not fully represent the charge movement in each domain (Campos et al., 2008). The guanidinium moiety of arginine, which is the charge center, can be as much 6–7 Å away from the backbone Cα carbon. Therefore, it is likely that the gating charges may contribute to currents that remain undetected by the S4 fluorophore (Campos et al., 2008).

Structural Implications on Interdomain Coupling in Voltage-dependent Ion Channels

The BrMT binding site on the Shaker potassium channel remains poorly defined. In comparison, functional evidence strongly suggests that the local anesthetic binds to the pore-lining residues in domains III and IV. Our data (Figs. 3, 6, and 7) also suggest that the binding of the local anesthetic to the pore affects the cooperativity between the voltage sensors of the sodium channel. Although we cannot rule out the possibility that the voltage sensors of the sodium channel interact with each other directly, we consider the alternative; namely, the interdomain cooperativity arises from coupling between the pore segments. Because the pore segments are themselves coupled to their corresponding voltage sensors, the voltage sensors of the different domains will be indirectly coupled. In the Shaker potassium channel, the final transition leading to channel opening is highly cooperative and may correspond to the splaying movement of the pore gates (Smith-Maxwell et al., 1998a,b; Ledwell and Aldrich, 1999; del Camino and Yellen, 2001). Nonetheless, there appears to be a fundamental difference between the gating mechanism of the Shaker potassium channel and the sodium channel. Several studies suggest that, unlike the sodium channel, the voltage sensors of the Shaker potassium

channel move independently of each other (Zagotta et al., 1994; Horn et al., 2000; Mannuzzu and Isacoff, 2000; Pathak et al., 2005).

We considered a simple model with interdomain coupling at the last transition in an attempt to account for our observations in the sodium channel (Fig. S2). This model is similar to the Zagotta-Aldrich-Hoshi model of gating of the Shaker potassium channel (Zagotta et al., 1994). Each subunit in this model undergoes two transitions: R→A and A→O. The two subunits (referred to as X and Y) in this hypothetical channel are coupled (n is the coupling term) to each other in the final step. If either one of the subunits enters the O state, it favors an A→O transition in the other subunit. This simple model is equivalent to the Zagotta-Aldrich-Hoshi model of gating of the Shaker potassium channel (Zagotta et al., 1994). The R state could correspond to S4 in the resting state, A to S4 in the activated state with S6 in the closed position, and O to S6 in the open position. Thus, the final concerted transition corresponds to the movement of the S6 gates.

The expressions describing the movements of each of the voltage sensors were derived analytically (see Materials and methods). We found that when the two subunits interact ($n = 10$), the equilibrium constants of the second transition (K_3 and K_4) play an important role in determining the steady-state behavior of the voltage sensors (F-V curves). When K_3 and K_4 favor forward transitions (K_3 and $K_4 \approx 10$), any perturbation in one domain resulted in the displacement of the F-V curve of the second domain (Fig. S3 and Table S1). On the other hand, when K_3 and K_4 favor reverse transitions (K_3 and $K_4 \approx 0.1$), the perturbations in one domain were not propagated to the second domain. This latter behavior is reminiscent of the effects seen in the Shaker potassium channel, whereas the earlier parameters generated a sodium channel–like behavior. These simulations show that the second transition may play a crucial role in isolating the cooperative interactions in the pore from propagating backward to the voltage-sensing segments. Although this second transition in our model corresponds to the movement of the S6 gates, it could equally well represent any of the intermediate transitions that link the voltage sensor movement to the opening of the pore gates. For instance, the strength of the coupling between the voltage sensor and S6 may determine whether the intersubunit coupling in the final transition propagates to the initial voltage-dependent transitions. This model allows us to understand how a limited change in a Shaker-like gating scheme can account for seemingly divergent behavior of the sodium and potassium channels.

Next, using the set of parameters that generates sodium channel–like behavior (K_3 and $K_4 = 10$), we consider whether the local anesthetic stabilizes the X_RY_A state ($K_3 = 10$ and $K_4 = 100$). This corresponds to stabilizing the S6 of subunit Y in the open position (Table IV). Fig. 8 shows that when the coupling is intact, this modification causes a hyperpolarizing shift in the voltage-dependent movement of both subunits X and Y (Fig. 8, left). When in addition to this modification the coupling is also eliminated ($n = 1$), the voltage dependence of the subunits shifts in the opposite direction relative to the shifts obtained before drug application (Fig. 8, right). The large leftward shift of subunit Y is similar to the local anesthetic effect on the movement of the S4 domain III, and the rightward shift of subunit X corresponds to those seen on the S4 domain I. Therefore, a simple model where the local anesthetic disrupts interdomain coupling and stabilizes one of the pore gates in the activated position can account for the most significant observation in our study.

TABLE IV

Parameters for F-V Curves in a Model System to Consider Two Possible Perturbations by the Local Anesthetic

	Case I		Case II	
	Subunit X	Subunit Y	Subunit X	Subunit Y
Coupling terms, n	10		10 ↓ 1	
Input V_m values	0	−50	0	−50
Input K_3 values	10	N/A	10	N/A
Input K_4 values	N/A	10 ↓ 100	N/A	10 ↓ 100
Output V_m values	−101.80 ↓ −112.92	−123.49 ↓ −170.37	−101.80 ↓ −60.67	−123.49 ↓ −166.76

K_1 and K_2 are determined by input V_m values and kept unchanged through these sets of simulations. The input K_3 and K_4 values determine the equilibrium of A→O transitions. As K_4 is increased, the S6 segment of subunit Y is stabilized in the activated position. In case II, the coupling term, n, was reduced along with the change in K_4. The output V_m values were calculated by fitting the simulated F-V relationships of subunits X and Y with a Boltzmann function.

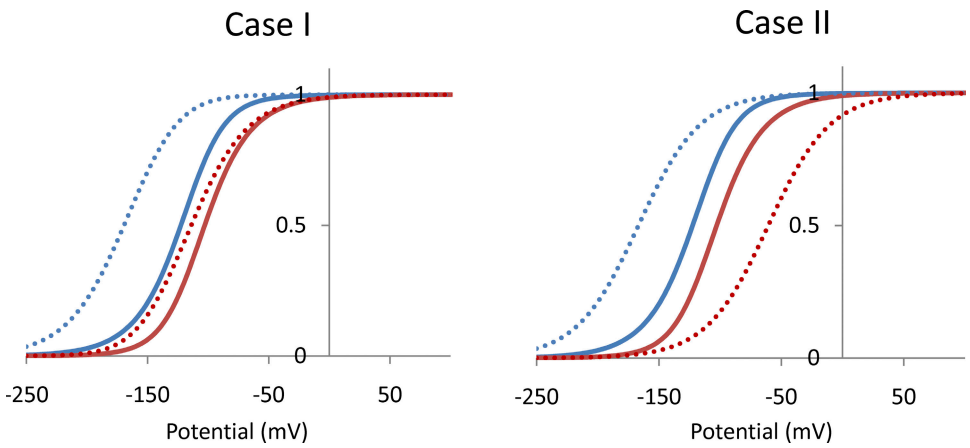

Figure 8. Simulations of F-V relationships in a simplified model system to consider two possible perturbations by the local anesthetic. Simulated F-V curves tracking the voltage sensor movement (R→A transition) in the two subunits of a hypothetical channel (Subunit X [red] and Subunit Y [blue]). (Left) The effect of a perturbation that stabilizes the open state (K_4 = 100) of the subunit Y while the coupling remains intact (n = 10) on the F-V curves of the two subunits (Case I). (Right) The effect of perturbations stabilizing the open state (K_4 = 100) of the subunit Y and disrupting the interdomain interaction (n = 1) on the F-V curves of the two subunits (Case II). Both panels show that the F-V curves before (solid lines) and after perturbation (dashed lines). All parameters are listed in Table IV.

A Possible Mechanism of Modulation of Voltage Sensors by Local Anesthetics

Finally, based on the available structural data and our findings, we propose a preliminary physical model to explain the modulation of voltage-dependent gating by local anesthetics. The structures of the open potassium channels show that these S6 helices are bent in the hinge region above the bundle crossing, which causes an outward splaying of these helices (Jiang et al., 2002). Molecular modeling of structure–function data show that the local anesthetic can bind to the channel only in an open conformation (Lipkind and Fozzard, 2005). Some of the critical residues involved in local anesthetic binding, such as Y1586 in Nav1.4 channels, are present near a region where the four S6 helices cross, referred to as the bundle crossing. From the structure of the closed state of the potassium channel, it is clear that residues of the four S6 segments interact intimately with each other at the bundle crossing (Doyle et al., 1998). Thus, it is unlikely that the channel can be fully closed when a local anesthetic is bound to the sodium channel. Because the local anesthetic binding site is only in

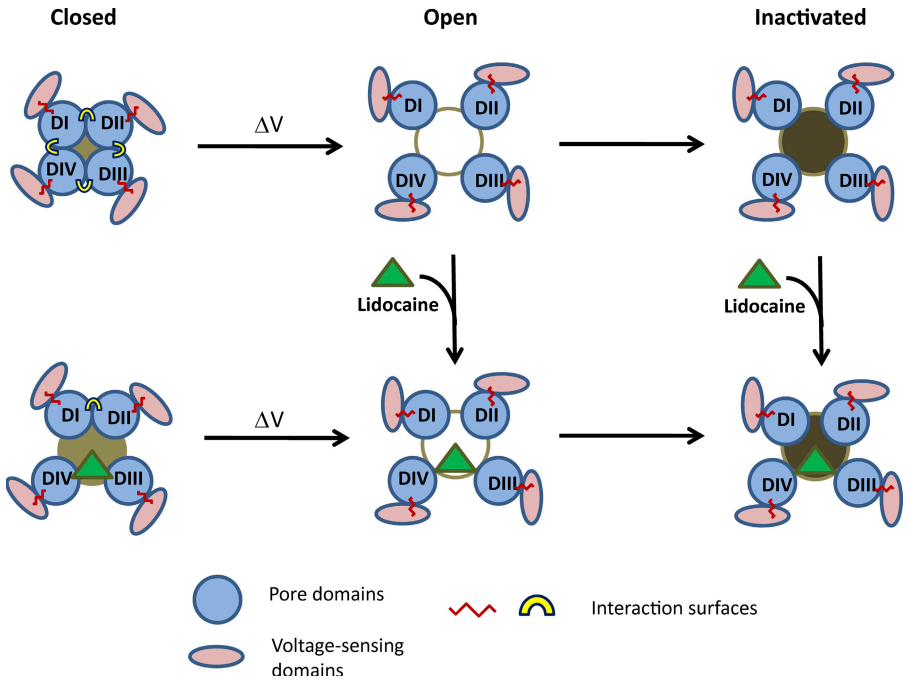

Figure 9. A schematic depicting a preliminary model of sodium channel modulation by local anesthetics. Local anesthetic binding to the open and inactivated state primarily stabilizes the pore segments of domain III and to some extent of domain IV in the open state. Because the movement of pore helices (blue circles) is coupled to the voltage sensor (pink ellipsoids), local anesthetic binding also stabilizes the voltage sensors of domains III and IV in the activated state. The interdomain interaction is mediated by the residues near the inner helix bundle crossing. In this model, as in the potassium channel, these residues interact in the closed state of the channel. This interaction is disrupted if the local anesthetic acts as a wedge and prevents the S6 segments of domains III and IV from fully closing.

domains III and IV, we propose that the S6 helices of these domains remain "stuck open" even upon repolarization (Fig. 9). This does not necessarily mean that the S6 segments of domains III and IV always remain in the same conformation as in their open state. Our data show that the voltage sensors of domains III and IV can return to a resting conformation when a strong force, namely large voltage, is applied, suggesting that their corresponding S6 segments are able to return to some sort of a closed conformation. Nonetheless, the important point here is that even when the S6 segments of domains III and IV return to a closed-like conformation, their interactions with the other S6 segments were disrupted. One possible scenario is that the S6 segments of domains III and IV do not return to a fully closed conformation in the presence of local anesthetic; consequently, their helices are less tightly packed at the bundle crossing. We postulate that local anesthetic acts as a wedge that keeps the S6 segments of domains III and IV from fully closing. This conformation of the channel may be the basis for less tightly coupled voltage sensors of the sodium channel in the presence of local anesthetics. Support for the view that the residues in the bundle crossing play an important role in intersubunit coupling comes from studies in the Shaker potassium channel (Yifrach and MacKinnon, 2002). Alanine-scanning mutagenesis in the S5-S6 segments shows that the residues lining the inner helix (S6) bundle crossing are involved in the final concerted opening transition. Most mutations in this region are likely to disrupt the packing and destabilize the inherently stable closed state. Our findings that local anesthetics disrupt interdomain cooperativity in the sodium channel are consistent with this emerging notion that the pore region of voltage-gated ion channels plays a central role in intersubunit interaction.

We thank members of the Chanda laboratory for discussions, M. Waldof for technical assistance, and Drs. M. Jackson, C. Czajkowski, and G. Robertson for their comments on an early version of this manuscript.

This project was supported by funds from the National Institutes of Health (GM084140-01), AHA Scientist Development Award (0535214N), and the Shaw Scientist award to B. Chanda.

Edward N. Pugh Jr. served as editor.

Submitted: 13 August 2008
Accepted: 21 November 2008

REFERENCES

Ahern, C.A., A.L. Eastwood, D.A. Dougherty, and R. Horn. 2008. Electrostatic contributions of aromatic residues in the local anesthetic receptor of voltage-gated sodium channels. *Circ. Res.* 102:86–94.

Armstrong, C.M. 1971. Interaction of tetraethylammonium ion derivatives with the potassium channels of giant axons. *J. Gen. Physiol.* 58:413–437.

Armstrong, C.M., and B. Hille. 1972. The inner quaternary ammonium ion receptor in potassium channels of the node of Ranvier. *J. Gen. Physiol.* 59:388–400.

Bezanilla, F., E. Perozo, D.M. Papazian, and E. Stefani. 1991. Molecular basis of gating charge immobilization in Shaker potassium channels. *Science.* 254:679–683.

Cahalan, M.D. 1978. Local anesthetic block of sodium channels in normal and pronase-treated squid giant axons. *Biophys. J.* 23:285–311.

Cahalan, M.D., and W. Almers. 1979. Interactions between quaternary lidocaine, the sodium channel gates, and tetrodotoxin. *Biophys. J.* 27:39–55.

Campos, F.V., B. Chanda, P.S. Beirao, and F. Bezanilla. 2007. β-Scorpion toxin modifies gating transitions in all four voltage sensors of the sodium channel. *J. Gen. Physiol.* 130:257–268.

Campos, F.V., B. Chanda, P.S. Beirao, and F. Bezanilla. 2008. α-Scorpion toxin impairs a conformational change that leads to fast inactivation of muscle sodium channels. *J. Gen. Physiol.* 132:251–263.

Cha, A., and F. Bezanilla. 1998. Structural implications of fluorescence quenching in the Shaker K^+ channel. *J. Gen. Physiol.* 112:391–408.

Chanda, B., and F. Bezanilla. 2002. Tracking voltage-dependent conformational changes in skeletal muscle sodium channel during activation. *J. Gen. Physiol.* 120:629–645.

Chanda, B., O.K. Asamoah, and F. Bezanilla. 2004. Coupling interactions between voltage sensors of the sodium channel as revealed by site-specific measurements. *J. Gen. Physiol.* 123:217–230.

Chen, L.Q., V. Santarelli, R. Horn, and R.G. Kallen. 1996. A unique role for the S4 segment of domain 4 in the inactivation of sodium channels. *J. Gen. Physiol.* 108:549–556.

del Camino, D., and G. Yellen. 2001. Tight steric closure at the intracellular activation gate of a voltage-gated K+ channel. *Neuron.* 32:649–656.

Doyle, D.A., C.J. Morais, R.A. Pfuetzner, A. Kuo, J.M. Gulbis, S.L. Cohen, B.T. Chait, and R. MacKinnon. 1998. The structure of the potassium channel: molecular basis of K+ conduction and selectivity. *Science.* 280:69–77.

Hanck, D.A., and M.F. Sheets. 1995. Modification of inactivation in cardiac sodium channels: ionic current studies with Anthopleurin-A toxin. *J. Gen. Physiol.* 106:601–616.

Hanck, D.A., J.C. Makielski, and M.F. Sheets. 1994. Kinetic effects of quaternary lidocaine block of cardiac sodium channels: a gating current study. *J. Gen. Physiol.* 103:19–43.

Hanck, D.A., J.C. Makielski, and M.F. Sheets. 2000. Lidocaine alters activation gating of cardiac Na channels. *Pflugers Arch.* 439:814–821.

Hille, B. 1977. Local anesthetics: hydrophilic and hydrophobic pathways for the drug-receptor reaction. *J. Gen. Physiol.* 69:497–515.

Horn, R., S. Ding, and H.J. Gruber. 2000. Immobilizing the moving parts of voltage-gated ion channels. *J. Gen. Physiol.* 116: 461–476.

Jiang, Y., A. Lee, J. Chen, M. Cadene, B.T. Chait, and R. MacKinnon. 2002. The open pore conformation of potassium channels. *Nature.* 417:523–526.

Koblin, D.D., W.D. Pace, and H.H. Wang. 1975. The penetration of local anesthetics into the red blood cell membrane as studied by fluorescence quenching. *Arch. Biochem. Biophys.* 171:176–182.

Kumbhakar, M., S. Nath, T. Mukherjee, and H. Pal. 2004. Intermolecular electron transfer between coumarin dyes and aromatic amines in Triton-X-100 micellar solutions: evidence for Marcus inverted region. *J. Chem. Phys.* 120:2824–2834.

Ledwell, J.L., and R.W. Aldrich. 1999. Mutations in the S4 region isolate the final voltage-dependent cooperative step in potassium channel activation. *J. Gen. Physiol.* 113:389–414.

Lipkind, G.M., and H.A. Fozzard. 2005. Molecular modeling of local anesthetic drug binding by voltage-gated sodium channels. *Mol. Pharmacol.* 68:1611–1622.

Makielski, J.C., J. Limberis, Z. Fan, and J.W. Kyle. 1999. Intrinsic lidocaine affinity for Na channels expressed in Xenopus oocytes depends on alpha (hH1 vs. rSkM1) and beta 1 subunits. *Cardiovasc. Res.* 42:503–509.

Mannuzzu, L.M., and E.Y. Isacoff. 2000. Independence and cooperativity in rearrangements of a potassium channel voltage sensor revealed by single subunit fluorescence. *J. Gen. Physiol.* 115:257–268.

Mannuzzu, L.M., M.M. Moronne, and E.Y. Isacoff. 1996. Direct physical measure of conformational rearrangement underlying potassium channel gating. *Science.* 271:213–216.

Pathak, M., L. Kurtz, F. Tombola, and E. Isacoff. 2005. The cooperative voltage sensor motion that gates a potassium channel. *J. Gen. Physiol.* 125:57–69.

Ragsdale, D.S., J.C. McPhee, T. Scheuer, and W.A. Catterall. 1994. Molecular determinants of state-dependent block of Na+ channels by local anesthetics. *Science.* 265:1724–1728.

Ragsdale, D.S., J.C. McPhee, T. Scheuer, and W.A. Catterall. 1996. Common molecular determinants of local anesthetic, antiarrhythmic, and anticonvulsant block of voltage-gated Na+ channels. *Proc. Natl. Acad. Sci. USA.* 93:9270–9275.

Rehm, D., and A. Weller. 1970. Kinetics of fluorescence quenching by electron and H-atom transfer. *Isr. J. Chem.* 8:259–271.

Sack, J.T., and R.W. Aldrich. 2006. Binding of a gating modifier toxin induces intersubunit cooperativity early in the Shaker K channel's activation pathway. *J. Gen. Physiol.* 128:119–132.

Schwarz, W., P.T. Palade, and B. Hille. 1977. Local anesthetics. Effect of pH on use-dependent block of sodium channels in frog muscle. *Biophys. J.* 20:343–368.

Sheets, M.F., and D.A. Hanck. 1995. Voltage-dependent open-state inactivation of cardiac sodium channels: gating current studies with Anthopleurin-A toxin. *J. Gen. Physiol.* 106:617–640.

Sheets, M.F., and D.A. Hanck. 2003. Molecular action of lidocaine on the voltage sensors of sodium channels. *J. Gen. Physiol.* 121:163–175.

Sheets, M.F., M.M. McNulty, T. Chen, and D. Hanck. 2008. Modification of gating differentiates rested state block from use-dependent block for lidocaine interactions with Na channels. *Biophys. J.* 94:3085.

Smith-Maxwell, C.J., J.L. Ledwell, and R.W. Aldrich. 1998a. Role of the S4 in cooperativity of voltage-dependent potassium channel activation. *J. Gen. Physiol.* 111:399–420.

Smith-Maxwell, C.J., J.L. Ledwell, and R.W. Aldrich. 1998b. Uncharged S4 residues and cooperativity in voltage-dependent potassium channel activation. *J. Gen. Physiol.* 111:421–439.

Strichartz, G.R. 1973. The inhibition of sodium currents in myelinated nerve by quaternary derivatives of lidocaine. *J. Gen. Physiol.* 62:37–57.

Vedantham, V., and S.C. Cannon. 1999. The position of the fast-inactivation gate during lidocaine block of voltage-gated Na^+ channels. *J. Gen. Physiol.* 113:7–16.

Wang, S.Y., M. Barile, and G.K. Wang. 2001. Disparate role of Na+ channel D2-S6 residues in batrachotoxin and local anesthetic action. *Mol. Pharmacol.* 59:1100–1107.

Yarov-Yarovoy, V., J. Brown, E.M. Sharp, J.J. Clare, T. Scheuer, and W.A. Catterall. 2001. Molecular determinants of voltage-dependent gating and binding of pore-blocking drugs in transmembrane segment IIIS6 of the Na(+) channel alpha subunit. *J. Biol. Chem.* 276:20–27.

Yarov-Yarovoy, V., J.C. McPhee, D. Idsvoog, C. Pate, T. Scheuer, and W.A. Catterall. 2002. Role of amino acid residues in transmembrane segments IS6 and IIS6 of the Na+ channel alpha subunit in voltage-dependent gating and drug block. *J. Biol. Chem.* 277:35393–35401.

Yifrach, O., and R. MacKinnon. 2002. Energetics of pore opening in a voltage-gated K(+) channel. *Cell.* 111:231–239.

Zagotta, W.N., T. Hoshi, and R.W. Aldrich. 1994. Shaker potassium channel gating. III: evaluation of kinetic models for activation. *J. Gen. Physiol.* 103:321–362.